Final publication is available from Biomed Mater. 2018;13(2):025021
https://doi.org/10.1088/1748-605X/aa9ad2

Generation of genipin cross-linked fibrin-agarose hydrogels tissue–like models for tissue engineering applications.

F. Campos[1], A.B. Bonhome-Espinosa[2], G. Vizcaíno [1,3], I.A. Rodríguez [1], D. Durand-Herrera[1], M.T. López-López[2], I. Sánchez-Montesinos[4]*, M. Alaminos[1], M.C. Sánchez-Quevedo[1]*, V. Carriel[1]*

Abstract
Generation of biomimetic and biocompatible artificial tissues is the basic research objective for tissue engineering (TE). In this sense, the biofabrication of scaffolds that resemble the tissues' extracellular matrix (ECM) is an essential aim in this field. Uncompressed and nanostructured fibrin-agarose hydrogels (FAH and NFAH respectively) emerged as promising scaffold in TE, but its structure and biomechanical properties must be improved in order to broad their TE applications. Here we generated and characterized novel membrane-like models with increased structural and biomechanical properties based on the chemical cross-linking of FAH and NFAH with genipin (GP at 0.1, 0.25, 0.5 and 0.75%). Furthermore, scaffolds were subjected to rheological (G, G', G" modulus), ultrastructural and *ex vivo* biocompatibility analyses. Results showed that all GP concentrations increased the stiffness (G) and especially the elasticity (G') of FAH and NFAH. Ultrastructural analyses demonstrated that GP and nanostructuration of FAH allowed controlling the porosity of FAH. In addition, biological studies revealed that higher concentration of GP significantly decreased the cell viability. Finally, this study demonstrated the possibility to generate natural FAH and NFAH with improved structural and biomechanical properties by using GP. However, further *in vivo* studies are needed in order to demonstrate the biocompatibility, biodegradability and regeneration capability of these cross-linked scaffolds.

Keywords
Tissue engineering — Nanostructuration technique — Genipin Cross-linking — Fibrin-agarose — Hydrogels — Cell-biomaterials interactions — Rheology

[1] *Department of Histology, Tissue Engineering Group, Faculty of Medicine, University of Granada and Instituto de Investigación Biosanitaria Ibs.GRANADA, Spain.*
[2] *Department of Applied Physics, Faculty of Science, University of Granada, Granada, Spain.*
[3] *Doctoral Program in Biomedicine, University of Granada, Spain.*
[4] *Department of Human Anatomy and Embryology, Faculty of Medicine, University of Granada, Granada, Spain.*
***Corresponding author**: mcsanchez@ugr.es, vcarriel@ugr.es

Contents

Introduction

Generation of biomimetic and biocompatible bio-artificial tissue-like substitutes is a basic research objective for tissue

engineering (TE) field. In this sense, the processes of biofabrication and functionalization of biomaterials for the generation of bio-artificial tissues, are a preferential research target in this field, since biomaterials are crucial components for biological and biomechanical properties as well as for their *in vivo* integration [1].

In TE the most used biomaterials are hydrogels, which are constituted by hydrophilic chains in which water is the dispersion medium. Hydrogels are generally composed by proteins or polysaccharides [2]. From protein-based hydrogels, the most commonly used biomaterials are fibrin, collagen and gelatin, while chitosan, alginate, cellulose, agarose and hyaluronic acid represent the most frequently used polysaccharides based ones [3].

In general hydrogels are biocompatible and could resemble the structure, hydration-rate and some biological and physical properties of the native extracellular matrix (ECM). Hydrogels support different cell functions (proliferation, migration and differentiation) and their hydration-rate allows the diffusion of nutrients and waste materials maintaining an adequate microenvironment. However, most hydrogels do not have optimal biomechanical behavior limiting their potential clinical applications [1, 4, 5]. Nowadays, these disadvantages can be solving by using physical (such as nanostructuration technique) or chemical methods (such as cross-linkers) that were used to improve the structural and biomechanical properties of different hydrogels. These methods allow tuning the structure and biomechanical properties of hydrogels according to specific needs [2, 6–9]. Nanostructuration is a physical method that induces nano-molecular bonds among the biomaterial fibrillar components improving the biomechanical forces and increasing the fibers density [9]. In the case of chemical cross-linkers they induce the formation of molecular interactions (cross-linking) between the biomaterial's molecular-units modifying their biomechanical and structural properties [7, 8, 10].

In recent years, a novel hybrid hydrogel composed of human fibrin and agarose type VII, fibrin-agarose hydrogel (FAH), has been used as scaffold to generate new bio-artificial tissues such as corneas, oral mucosa, skin, peripheral nerve, cartilage, palate and magnetic scaffolds with promising *in vitro* and *in vivo* results [9, 11–17]. These previous studies demonstrated that FAH-based bio-artificial tissue-like models were highly biocompatible, biodegradable and supported cell functions. In addition, overall biomechanical and structural properties of this versatile FAH were significantly improved by using nanostructuration technique [2, 8, 9], generating nanostructured FAH (NFAH). Furthermore, the protein/polysaccharide hybrid composition of FAH and NFAH made them suitable targets for chemical cross-linkers [8].

Glutaraldehyde (GL) is probably one of the most efficient cross-linkers used in biomedicine, but studies demonstrated some cytotoxic effects of this agent, especially at higher concentrations [8, 18]. In our previous study, significant improvements of overall biomechanical properties of FAH and NFAH were obtained with GL. Although, at higher concentrations of GL the cell viability and functionally decreased considerably [8]. Despite the improvements obtained with GL, it is still necessary to find none or less toxic cross-linkers agents to improve the physical and biological properties of FAH and NFAH for TE applications. In this context, genipin (GP) appeared as a possible alternative for this issue. For more than a decade, GP, an iridoid glycoside (C11H14O5), has been applied as a cross-linker agent to decellularized tissues (Somers et al., 2008), chitosan, collagen, gelatin, polyethylene glycol and fibrin hydrogels with some biomechanical improvements and lower levels of cytotoxicity as compared to GL [19, 20]. In this context, the aim of this study was to generate and characterize novel FAH and NFAH membrane-like scaffolds with improved structural and biomechanical properties by using different concentration of GP as cross-linker. Furthermore, the generated GP cross-linked scaffolds were subjected to structural, rheological and *ex vivo* biocompatibility analyses to confirm their potential usefulness in TE.

1. Methods

1.1 Generation of uncompressed and nanostructured fibrin-agarose hydrogels

In this study, FAH and NFAH were elaborated by following well-described protocols [8, 9, 12, 16]. To prepare 30 ml FAH, we mixed 22.8 ml human plasma, 2.25 ml PBS and 450 μl of an anti-fibrinolytic (Amchafibrin, Fides-Ecofarma, Valencia, Spain). Once the solution was mixed, 3 ml of 2% $CaCl_2$ (to promote the gelation) and 1.5 ml melted of 2% type VII-agarose (Sigma-Aldrich, Steinheim, Germany) were added, carefully mixed and placed into 6-wells plates (3.5 cm diameter with 5 ml in each) and leaved to jellified during 1 h under standard culture conditions (37ºC and 5% CO_2).

To fabricate NFAH, constructs were carefully removed from each well plate and subjected to plastic compression techniques following previously described and standardized procedures [8, 9]. Briefly, we placed the FAH between a couple of nylon filter membranes with 0.22 μm pore size (Merck-Millipore, Darmstadt, Germany) and compressed them between a pair of sterile Whatman 3 mm absorbent pieces of paper below a flat glass surface. We applied uniform mechanical pressure (500 g, homogeneously distributed) for 3 min and, as results, we obtained a high-density membrane-like NFAH (film) with approximately 50-60 μm thickness.

1.2 Genipin cross-linking and experimental groups

To improve the structural and biomechanical properties of FAH and NFAH, constructs were subjected to chemical cross-linking with GP at 0.1%, 0.25%, 0.5% and 0.75% (w/v) diluted in PBS in bath water at 37ºC (0.1 M, pH 7, 2-7, 4). In this study, constructs were submerged in 5 ml of GP solutions for 72 hours at 37ºC in darkness. After this period, cross-linked constructs were washed during 24 hours with PBS. In the present work eight experimental groups were defined based on the type of hydrogel (FAH or NFAH) and four GP

concentrations. Not cross-linked FAH and NFAH were used as control. Finally, all experimental and control groups were analyzed in triplicate throughout this study (n=3 in each).

1.3 Scanning electron microscopy

For these analyses, GP cross-linked FAH and NFAH and controls were fixed in 2.5% glutaraldehyde cacodylate-buffered and postfixed in 1% osmium tetroxide. After fixation, samples were dehydrated in increasing concentrations of acetone (30-100%), subjected to critical point dry, mounted on aluminum stubs and coated with gold according to routine procedures [9]. Samples were analyzed with a FEI Quanta 200 environmental scanning electron microscope (FEI Europe, Eindhoven, The Netherlands).

1.4 Quantitative analysis of biomaterial's porosity

In this study the porosity and fibers density was determined in cross-linked and control scaffolds through the analysis of SEM images with Image J software (National Institutes of Health, USA) as previously described [8, 14, 21]. Briefly, 6 SEM images from three independent samples (from each biomaterials condition) were processed in Image J with the threshold function by default setting and selecting the dark background (obtaining black/white SEM images). In set measurements tolls we selected the "area fraction" function and then automatically calculated the percentage of black and white elements present in a specific area. The percentage of black areas in each image corresponded to the fiber-free area, thus the biomaterials' porosity. The fibers density, which was represented in white, was calculated as the difference between total analyzed area and the percentage of porosity (black). See representative modified images in Supplementary material (Fig S. 1). Finally, results were expressed as mean ± standard deviation (SD) values for both variables in the experimental and control groups.

1.5 Rheological characterization

In order to demonstrate the impact of GP cross-linking on scaffolds' biomechanical properties all scaffolds generated were subjected to a stationary and dynamic rheological analysis as described previously [8, 22, 23]. Briefly, hydrogels of 5 mm thickness and 30 mm diameter were analyzed in a Haake MARS III rheometer (Thermo Fisher Scientific, USA). Stationary rheological analyses were used to determine the rigidity modulus (G), whereas the analyses carried out under dynamic state displayed the elastic and viscous modules (G' and G" respectively). Cross-linked and controls scaffolds were analyzed in triplicate and under the same environmental conditions (37 ± 1 ºC).

1.6 *Ex vivo* biocompatibility

In this study human skin fibroblasts were used to determine *ex vivo* biocompatibility of the different constructs generated. Cells were isolated from skin biopsies of healthy donors as described previously [15]. Fibroblasts were expanded until passage 5 with DMEM (supplemented with 5% antibiotics cocktail solution and 10% fetal bovine serum, all from Sigma Aldrich, Germany) under standard culture conditions. In order to determine the biocompatibility *ex vivo*, cells were seeded on top of each construct (10^4 cells/construct or chamber), kept under standard culture conditions during 48h and then subjected to the following tests: (i) Live/Dead® (LD) cell viability assay, (ii) Determination of mitochondrial dehydrogenase activity (WST-1) and (iii) DNA quantification assay. As technical positive controls, cells were cultured at the same density on top of non-cross-linked constructs and in chamber slides (2D) for 48h. In addition, cells cultured in chamber slides for 48h and then incubated with 2% Triton X-100 were used as technical 2D negative control. Furthermore, all analyses were performed in triplicate, unless otherwise is indicated.

For LD cell viability assay we followed the manufacture recommendations (Viability/Cytotoxicity kit, Molecular probes, Eugene, Oregon, USA) and previous studies [8, 16] . Briefly, the culture medium was removed from constructs and chamber slides followed by three washed with PBS (5 min each) and finally samples were incubated with working solution (acetomethoxy-calcein and ethidium bromide) for 30 min. After that the solution was removed, samples were washed in PBS and viable (green fluorescence) and dead cells (red fluorescence) were analyzed by fluorescence microscopy (Nikon Eclipse Ti-U fluorescence and light inverted microscope, Nikon, Tokyo, Japan). Furthermore, the cell density in each GP cross-linked FAH and controls (FAH and 2D positive control) was determined as the number of cells/analyzed area (total area: 101.5 x 10^4 μm^2).

The metabolic activity of fibroblast was quantitatively determined with the water-soluble tetrazolium salt-1 (WST-1) colorimetric assay following the manufacturing (Cell Proliferation Reagent WST-1, Roche Diagnostics, Mannheim, Germany) and previously described recommendations [8, 23]. Finally, the nuclear membrane permeability, which is considered a feasible test of irreversible cell damaged, was evaluated by the quantification of DNA released into the culture medium as described previously [8, 22, 23]. In this sense, the culture media was harvested from each condition, placed in Eppendorf tubes and the DNA was quantified by using a NanoDrop 2000 UV-Vis Spectrophotometer (Thermo Fisher Scientific). The DNA was quantified in four independent samples from each experimental condition, and three measurements were made in each (n = 12 each). In addition to the controls described above (2D positive and negative), we determined the DNA content in the culture medium and these values were subtracted from the results obtained from each experimental condition and control.

Finally, all quantitative results obtained from the *ex vivo* biocompatibility analyses were expressed as mean ± standard deviation (SD) values, which in the case of WST-1 and DNA were normalized with their respective controls.

1.7 Quantitative and Statistical Analysis

To determine statistically significant differences between the comparison of different variables obtained from each experimental condition and control, all variables (values) were first subjected to the Shapiro-Wilk test for normality. In this sense, student's t-test was used to compare area fraction (porosity) and fiber density values, while values of WST-1, DNA, cell density and G, G' and G" modules were compared with Mann-Whitney test. In addition, the Kendall rank correlation test was used to determine the statistically significant positive or negative correlations between WST-1 and DNA values. All data were analyzed with SPSS 16.00 and values p¡0.05 were considered statistically significant in two toiled test.

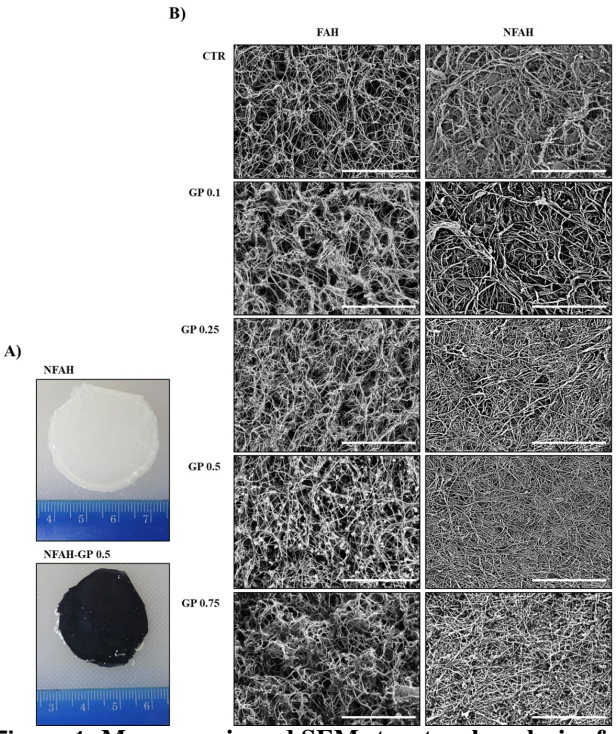

Figure 1. Macroscopic and SEM structural analysis of FAH, NFAH and GP cross-linked scaffolds. A) Shows the representative macroscopic appearance of NFAH (control) with their characteristic white color and one of the most adequate and representative GP cross-linked NFAH (GP 0.5) of this study with their typical colorimetric blue reaction. **B)** SEM representative images of FA-based hydrogels, where it is possible to identify their characteristic porous and fibrillar pattern, which was modified by the nanostructuration process and in function of the use of different concentrations of GP. Scale bar= 20 μm.

2. Results

2.1 Colorimetric reaction and structural scanning electron microscopy

The macroscopic appearance of FAH was characterized by a homogeneous white color, whereas, after the cross-linking with GP the characteristic colorimetric blue reaction was obtained (Fig. 1A).

The qualitative structural SEM characterization revealed the typical randomly oriented fibrillar and porous pattern of FAH and NFAH, which was preserved with slight structural modifications in GP cross-linked hydrogels (Fig. 1). This analysis confirmed that the nanostructuration technique increased the fiber density and reduces the scaffolds' porosity of FAH and NFAH. Interestingly, the increase of GP concentration (from 0.25% to 0.75%) induced some structural changes in both FAH and NFAH. These changes were characterized by an increase of the scaffold's fiber density and a reduction of the FAH, and especially NFAH's porosity. Finally, this analysis demonstrated that the nanostructuration of FAH followed by the cross-linking with GP 0.25-0.75 resulted in more dense and less porous scaffolds as compared to FAH and cross-linked FAH (Fig. 1).

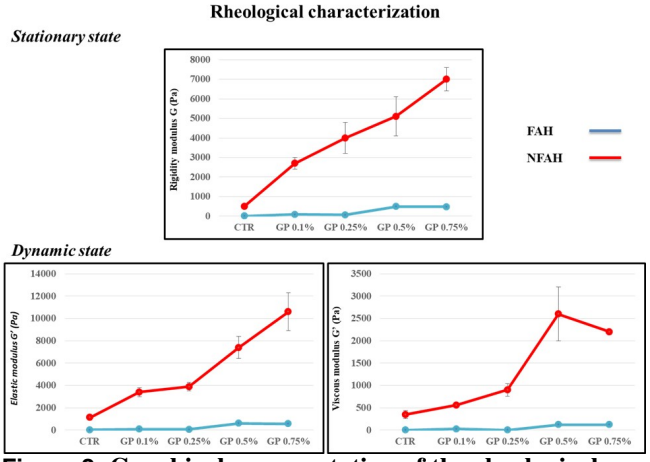

Figure 2. Graphical representation of the rheological characterization of FAH, NFAH and GP cross-linked scaffolds. Up: rigidity modulus, representing the initial slope of the shear stress vs. shear strain curve obtained under stationary conditions. Left: Elastic (storage) modulus, corresponding to the mean value of the linear viscoelastic region of amplitude sweeps at constant frequency of 1 Hz. Right: Viscous (loss) modulus corresponding to the mean value of the linear viscoelastic region of amplitude sweeps at constant frequency of 1 Hz.

When we performed quantitative analyses of scaffolds' porosity and fibers density we confirmed the findings observed by the qualitative structural analyses (Table 1). This analysis demonstrated that the nanostructuration of FAH to generate NFAH significantly reduced the porosity (from 65.27% to 49.24%) and increased the fiber density (34.73% to 50.76%), with a difference of 16.03% for both parameters (p¡0.05 for both). The detailed analysis of the impact of GP cross-linking into the structural properties of FAH showed that the increase of GP-concentration decreased the overall porosity (from 65.27% to 41.63%) and proportionally increased the fibers density (from 34.73%-58.37%) of FAH in a 23.64%. Most

	Scaffolds	CTR	GP 0.1%	GP 0.25%	GP 0.5%	GP 0.75%
POROSITY (%)	**FAH**	65.27 ± 5.23	56.22 ± 4.183[a,e]	53.48 ± 10.71[a,e]	46.03 ± 5.22[a,b,c,e]	41.63 ± 4.94[a,b,c,d]
	NFAH	49.24 ± 4.53[e]	48.75 ± 3.73	46.88 ± 2.70	40.77 ± 3.29[a,b,c]	39.69 ± 7.15[a,b,c]
FIBERS DENSITY (%)	**FAH**	34.73 ± 5.22	43.78 ± 4.183[a,e]	46.51 ± 10.71[a,e]	53.97 ± 5.22[a,b,c,e]	58.37 ± 4.94[a,b,c,d]
	NFAH	50.76 ± 4.53[e]	51.25 ± 3.73	53.11 ± 2.70	59.23 ± 3.29[a,b,c]	60.31 ± 7.15[a,b,c]

Table 1. Quantitative and statistical results of scaffolds' porosity and fibers density. In this table values corresponds to the percentage of porosity and fibers density of each biomaterials generated, and this values are shown as the mean ± standard deviation values. Statistical comparisons were made with Student's t-test and p¿0.05 were considered statistically significant. Letters indicate the significant differences for each comparison: [a]=Indicate significant differences of each experimental condition as compared to their non-cross-linked control (CTR). [b]=Indicate significant differences between GP 0.25; 0.5; 0.75% vs. GP 0.1% in each. [c]=Significant differences between GP 0.5% and 0.75% vs. GP 0.25% in each. [d]=Significant differences between GP 0.5% vs GP 0.75% in each. [e]=Significant differences between FAH vs NFAH for controls and each experimental condition.

differences between FAH and cross-linked FAH were statistically significant, except for comparison between GP 0.1% and GP 0.25% (p¿0.05). Similarly, the cross-linking of NFAH with GP also induced a reduction of scaffolds porosity accompanied by a proportional increase of fibers density in a 9.55% (Table 1). These differences were statistically significant when GP 0.5% and 0.75% were compared to control, GP 0.1% and GP 0.25%, but differences between GP 0.25% vs. GP 0.1% and GP 0.5% vs. GP 0.75% were not statistically significant (p¿0.05). Finally, this analysis confirmed that GP cross-linked NFAH were significantly less porous and denser than FAH for GP at 0.1 to 0.5% (p¡0.05). Curiously, differences between FAH and NFAH cross-linked with GP 0.75% were not statistically significant (p¿0.05) (Table 1).

2.2 Rheological characterization

Stationary state characterization of cross-linked scaffolds and controls revealed the increase of G values (rigidity modulus) due to the nanostructuration technique, GP cross-linking and by the combination of both (cross-linked NFAH) (Fig. 2 and Table 2). First, this analysis revealed that the nanostructuration of FAH to generate NFAH significantly increased G values (p¡0.05) in 468.5 Pa (starting from 31.5 to 500 Pa). When ascending concentrations of GP were used with FAH, G values were significantly increased as compared to controls (p¡0.05), and maximum G values (470 Pa) were obtained with GP 0.75% (Fig. 2 and Table 2). However, differences between FAH-GP 0.5% vs. FAH-GP 0.75% were not statistically significant (p¿0.05). Interestingly, the combination of nanostructuration with GP cross-linking resulted in the generation of cross-linked NFAH with significantly superior (p¡0.05) G values as compared to non-cross-linked and cross-linked FAH (Fig. 2 and Table 2). The increase of these values from 500 Pa (NFAH) to 7000 Pa (NFAH GP 0.75%) was related to the increase GP concentration, and most of these differences were statistically significant (p¡0.05), except the comparison between NFAH-GP 0.5% vs. NFAH-GP 0.25% (p=0.081).

Dynamic state analyses of the G' (elastic modulus) and G" (viscous modulus) showed similar trend with G values. In this regard, NFAH showed significantly higher G' and G" values (p¡0.05) as compared to FAH (Fig. 2 and Table 2). The cross-linking of FAH with ascending concentrations of GP resulted in an increase of G' (from 36 Pa to 610 Pa) and G" (8.9 Pa to 124 Pa) values when GP 0.1% to GP 0.5% were used (Fig. 2 and Table 2), and all these values were significantly higher than non-cross-linked FAH (p¡0.05). Curiously, the use of GP 0.75% resulted in a slight and not significant reduction of G' and G" values as compared to GP 0.5% (p¿0.05). Finally, these analyses demonstrated that the GP cross-linking of NFAH resulted in a significant increase of G' and G" values as compared to non-cross-linked NFAH and cross-linked FAH (Fig. 2 and Table 2) (p¡0.05). In the case of G' values, they increased in function of GP concentration, but G" values increased from GP 0.1% to GP 0.5% and a significant decrease was observed when GP 0.75% was used (p= 0.372).

2.3 *Ex vivo* biocompatibility

The functional and morphological analysis carried out with L/D assay demonstrated that viable cells (green fluorescence) were able to grow and attach to the FAH and cross-linked FAH (Fig. 3). In cross-linked FAH elongated and stellated cells were observed attached to the surface with comparable morphology to the 2D positive control. Interestingly, the cross-linking of FAH with GP at 0.1%, 0.25% and 0.5% did not affect the attachment of the cells to the scaffold surface. Furthermore, cells showed a comparable morphology to the FAH and 2D positive control (Fig. 3A). Nevertheless, the cross-linked of FAH with 0.75% GP resulted in an important decrease of the number of attached cells (Fig. 3). In this analysis we did not observe any dead cells (red fluorescence) in FAH and cross-linked FAH, probably because dead cells do not attach to the scaffolds and they were removed during the washing. However, dead cells were evident in the 2D negative control (2% Triton X-100) (Fig. 3A). The quantitative

	Scaffolds	CTR	GP 0.1%	GP 0.25%	GP 0.5%	GP 0.75%
G (Pa)	**FAH**	31.5 ± 2.3	84 ± 8[a,e]	65 ± 4[a,b,e]	490 ± 9[a,b,c,e]	470 ± 120[a,b,c,e]
	NFAH	500 ± 60[e]	2700 ± 300[a]	4000 ± 800[a,b]	5100 ± 1000[a,b]	7000 ± 600[a,b,c,d]
G' (Pa)	**FAH**	36 ± 7	93 ± 8[a,e]	74 ± 8[a,b,e]	610 ± 40[a,b,c,e]	570 ± 160[a,b,c,e]
	NFAH	1130 ± 220[e]	3400 ±400[a]	3900 ± 400[a,b]	7400 ± 1000[a,b,c]	10600 ± 1700[a,b,c,d]
G"(Pa)	**FAH**	8.9 ± 1.7	25 ± 3[a]	10.3 ± 1[a,b,e]	124 ± 8[a,b,c,e]	121 ± 19[a,b,c,e]
	NFAH	350 ± 90[e]	560 ± 40[a, e]	900 ± 140[a,b]	2600 ± 600[a,b,c]	2200 ± 60[a,b,c,d]

Table 2. Rheological static and dynamic statistical results. Quantitative results for each rheological test are shown as mean ± SD values. P¡0.05 were considered statistically significant for Mann-Whitney non-parametric test, and comparison between groups are indicate as follow: [a]=Indicate significant differences of each experimental condition as compared to their non-cross-linked control (CTR). [b]=Indicate significant differences between GP 0.25; 0.5; 0.75% vs. GP 0.1% in each. [c]=Significant differences between GP 0.5% and 0.75% vs. GP 0.25% in each. [d]=Significant differences between GP 0.5% vs GP 0.75% in each. [e]=Significant differences between FAH vs NFAH for controls and each experimental condition.

analysis of the cell density confirmed a significant decrease (p¡0.05) of these values when cells were seeded on FAH and GP cross-linked FAH as compared to the 2D positive control (Fig. 3B). When we compared these values between experimental conditions, significantly higher values were observed in FAH as compared to FAH cross-linked with GP 0.25-0.75% (p¡0.05), but not between FAH and FAH-GP 0.1 (p=0.209). Curiously, although a slight decrease of the cell density was observed between GP 0.1 to 0.5 cross-linked hydrogels, these differences were not statistically significant (p¿0.05). Finally, the use of GP 0.75% resulted in significantly lower values than the other GP cross-linked FAH (Fig. 3B).

The biochemical analysis of cells metabolic activity carried out with WST-1 assay showed significantly higher values (p¡0.05) in FAH group than the cross-linked FAH groups (Fig. 4). When we compared cells cultured on top of FAH and cross-linked FAH with 2D positive and negative controls all differences were statistically significant (p¡0.05). The analysis of cross-linked FAH revealed decrease of these values in function of the increase of GP concentrations (Fig. 4). Most of these differences were significant (p¡0.05), except the comparison between FAH-GP 0.25 vs. FAH-GP 0.5 (p=0.566).

The spectrophotometric analysis of DNA release (irreversible nuclear membrane damage) revealed the impact of the concentration of GP in the cell viability (Fig. 4). In 2D positive controls, DNA was not released into the culture media (0%), while 100% of DNA was released in the 2D negative control (2% Triton X-100). In this study, cells cultured into FAH and cross-linked FAH showed significant higher values than the 2D positive control (p¡0.05) and significantly lower than the 2D negative control (p¡0.05). Interestingly, the increase of GP concentration resulted in a progressive and significant increase of the percentage of DNA released (p¡0.05) from cells. In this study, maximum values of DNA released were found in GP .075%. However, there were no significant differences between FAH-GP 0.5 vs. FAH-GP 0.75 (p=0.401). Although the use of GP resulted in a significant release of DNA, these values represented less than 15% of the total DNA as compared to the 2D negative control (Fig. 4). Finally, Kendall's rank correlation test showed a negative correlation between WST-1 values and DNA-release values (p=0.000 and correlation coefficient r= -0.323).

3. Discussion

In this study we have developed two different tissue–like models composed of FAH and NFAH biomaterials subjected to the action of different concentrations of GP. The structural pattern, the mechanical behavior and the biocompatibility were investigated in these tissue–like models to determine their potential use in tissue engineering and regenerative medicine.

Concerning the possible mechanism of action of GP with our hybrid FA-based hydrogels, it could be supported by previous studies where the interaction of GP with fibrin [24] and agarose [25] was demonstrated. In the case of fibrin, it was suggested that two carbonyl functional groups of GP could react with free primary amines present in fibrin stablishing covalent bonds between fibrin macromolecules, with a characteristic visible colorimetric dark blue reaction [24]. Fibrin's GP cross-links impart increased biomechanical properties and attenuate the enzyme-mediate *in vitro* degradation [24]. In the case of agarose, it was suggested that GP could react with an small fraction of amino acid and therefore free amines present within agarose (around 0.25%) [25]. These interactions resulted in an increase of both the thermal stability and swelling ability of agarose hydrogels which was accompanied by the colorimetric blue reaction [25]. In this context, our FAH and NFAH were successfully cross-linked with GP and the typical dark blue colorimetric reaction was obtained. Concerning the mechanism of action, surely GP mainly interacted with

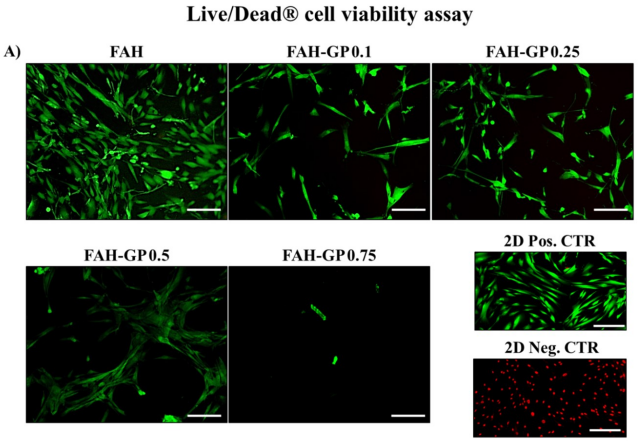

B)

	Controls		Genipin cross-linked FAH			
	2D Pos.	FAH	GP 0.1	GP 0.25	GP 0.5	GP 0.75
Cells/µm²	130 ± 7.34	95 ± 2.14	74 ± 5.46 a	67 ± 1.96 a,b	64 ± 2.3 a,b	1 ± 0.1 a,b,c,d,e

Figure 3. Human fibroblast behavior in FAH and GP cross-linked FAH. A) Live/Dead cell viability assay showing viable cells in green and dead cells in red, which are evident in cells treated with Triton X-100 (2D negative control). Scale bar= 100 μm. **B)** Quantitative results of the number of cells (or cell density) in controls (FAH and 2D positive) and GP cross-linked FAH. Values are shown as mean ± standard deviation of the cell number by analyzed area (101.5 x 104 μm2). P¡0.05 were considered statistically significant for Mann-Whitney non-parametric test, and comparison between groups are indicate as follow: a= Indicate statistically significant differences vs. 2D positive control (2D Pos.). b= Indicate statistically significant differences between GP cross-linked hydrogels vs. FAH. c= Indicate statistically significant differences between FAH-GP 0.25-0.75 vs. FAH-GP 0.1. d= Indicate statistically significant differences between FAH-GP 0.5 and 0.75 vs. FAH-GP 0.25. e= Indicate statistically significant differences between FAH-GP 0.5 vs. FAH-GP 0.75.

the free amines of fibrin and less with the small fraction of amino acid that could be present in the agarose, because our FA-based hydrogels were composed by 70% of fibrin and only 0.1% of agarose.

Our study demonstrated that GP cross-linked tissue-like FAH and NFAH preserved the porous and randomly oriented fibrillar pattern observed in non-cross-linked FAH and NFAH. There exists however significant differences among those patterns when different concentrations of GP were used. Scaffolds' porosity is an important issue in tissue engineering because it favors cell attachment, migration and proliferation. In this context, it was demonstrated that cell migration velocity across biomaterials was closely related to the pore size and their interconnected 3D organization [5]. In addition, biomaterials porosity has an impact on cell behavior and viability. Previous studies conducted with highly dense and compacted collagen hydrogels demonstrated that this 3D pattern compromised the diffusion of O^2, thus the cell functions and viability [26]. Similarly, highly dense and multilayered 3D organization of FAH resulted in a partial compromised of cell viability and functionally *ex vivo* [9]. These studies demonstrated that and adequate scaffold porosity is essential to provide a suitable microenvironment for nutrients and wastes diffusion, which are critical for the normal cell functions and tissue regeneration *in vivo* [**?**, 9, 13].

Our structural analyses demonstrated that FAH were the most porous scaffolds with lower fibrillar density. In contrast, the NFAH and especially the GP cross-linked scaffolds resulted in a significant reduction of the scaffolds' porosity and an increase of the fibers densities. These results demonstrate that using different concentrations of GP (between 0.1-0.75%) it is possible to modulate the degree of porosity and fibers densities of FAH and NFAH. Curiously, the action of GP into the structural properties of FAH (a difference of 16.03%) was more evident than in NFAH (a difference of 9.5%). These results could be explained by the lower compression capability of NFAH as compared to FAH [2, 8]. GP as other cross-linked agents induce molecular interactions into the scaffolds' fibers that result in different degrees of shrinkage. In addition, the nanostructuration technique is a physical method that induces a comparable effect [2]. Therefore, the range of shrinkage and

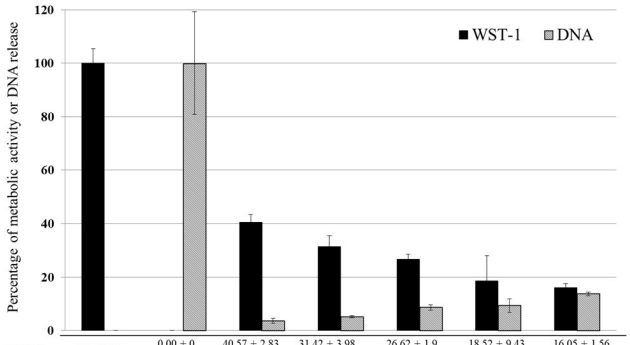

	CTR +	CTR -	FAH	GP 0.1	GP 0.25	GP 0.5	GP 0.75
	2D controls			GP cross-linked FAH			
WST-1	100 ± 5.43	0.00 ± 0 a	40.57 ± 2.83 a,b	31.42 ± 3.98 a,b,c	26.62 ± 1.9 a,b,c,d	18.52 ± 9.43 a,b,c,d	16.05 ± 1.56 a,b,c,d,e,f
DNA	0.00 ± 0	100 ± 19.2 a	3.57 ± 0.92 a,b	5.19 ± 0.47 a,b,c	8.60 ± 1.03 a,b,c,d	9.27 ± 2.54 a,b,c,d,e	13.69 ± 0.67 a,b,c,d,e

Figure 4. *Ex vivo* results of quantitative biocompatibility. Graphic and numeric representation of normalized values for WST-1 assay and DNA release for each 2D controls, FAH and GP cross-linked FAH. Numeric values are shown as mean ± SD, P¡0.05 were considered statistically significant for Mann-Whitney non-parametric test, and comparison between groups are indicate as follow: a= Indicate significant differences of each experimental condition as compared to CTR +. b= Indicate significant differences of each experimental condition as compared to CTR -. c= Indicate significant differences between GP cross-linked FAH vs. FAH in each. d= Indicate significant differences between GP 0.25; 0.5; 0.75% vs. GP 0.1% in each. e= Indicate significant differences between GP 0.5 and 0.75% vs GP 0.25% in each. f= Indicate ignificant differences between GP 0.5% vs GP 0.75%.

swelling capability of NFAH is reduced [8]. Similar findings were described by the use of other cross-linking agents [18,27]. Finally, based on these results the combination of a variable concentration of GP and/or nanostructuration techniques allowed an efficient control of the porosity in FAH scaffolds. Consequently, a correlation between the biomaterial and the cell type to be used in the elaboration of artificial tissues is possible [5, 28] . This will contribute to select the more appropriate structural properties for the specific application. Although GP has demonstrated to improve the biomechanical properties of different biomaterials [10, 20], it is important to investigate the effects of GP on the biomechanical properties of FAH and NFAH. Previous studies of our group have been demonstrated that it is possible to modulate the biomechanical properties and hydration rate of FAH by varying the agarose content and with the nanostructuration technique [2]. However, the biomechanical properties obtained through this approach resulted in lower values than those reported in literature for some native tissues (cartilage or skin) [2, 27, 29] limiting the biomedical applications of these FAH-based scaffolds.

The steady-state rheological analysis carried out in this study showed that the rigidity modulus (G) of FAH and NFAH was significantly improved with the use of different concentrations of GP as compared to non-cross-linked tissue-like scaffolds and to previously described results [2, 8]. Similarly, the dynamic state rheological analysis demonstrated that GP significantly improve the elastic modulus (G') and the viscous modulus (G") of both hydrogels, especially in the NFAH. Interestingly, our results demonstrated that the cross-linking of FAH and NFAH with GP resulted in four times higher elastic and viscous modulus (G' and G" respectively), indicating that these new tissue-like cross-linked scaffolds have clearly better elastic properties. Based on the structural and rheological characterization, it is possible to conclude that the rational combination of GP and nanostructuration technique is a feasible approach to generate customized scaffolds with improved biomechanical and structural properties. The cross-linking of NFAH with GP 0.5% resulted in comparable biomechanical properties than the obtained with the use of GL 0.25% [8], thus GP resulted to be an efficient alternative to the use of GL within FA-based hydrogels. This new generation of customized scaffolds could be designed with specific dimensions, porosity and rheological properties for tissue-specific applications (e.g. skin, cornea) or for the generation of different kind of biomedical devices such as membranes and conduits for peripheral nerve repair [13, 27, 30].

Although GP is generally accepted as a low toxicity cross-linking agent, especially compared to GL [24], some authors have described dose-dependent toxic effects of GP in different biomaterials in tissue engineering [19, 31, 32]. The evaluation of the *ex vivo* biocompatibility carried out at the morphological, biofunctional and biochemical levels (L/D, WST-1 and DNA release) demonstrated a concentration-dependent cytotoxicity of GP in human cells cultured in the GP cross-linked scaffolds.

The analysis of attached viable cells with L/D demonstrated that FAH and GP-cross-linked FAH supported cell attachment. However, quantitative analysis demonstrated a reduction of the cell density when fibroblasts were seeded on top of FAH and in GP cross-linked FAH. The reduction observed in non-cross-linked FAH could be explained by that fact that agarose reduces the cells adhesion function [33]. In the case of GP cross-linked FAH the decrease was in function of the GP-concentration used and differences among GP 0.1-0.5% were not statistically significant, and only a significant decreased was observed in FAH cross-linked with 0.75% of GP. These results are in agreement with previous studies were a decrease of the number of cells was observed in GP-cross-linked collagen hydrogels [34]. Curiously, no dead or spheroid-shape cells were observed in our study, which were observed when FAH were cross-linked with GL [8], or within GP-cross-linked fibrin hydrogels [35]. The absence of dead or spheroid cells in the present study could be related to the inability of dead cells to attach to the scaffold surface and therefore, they were removed during the washing process. In relation to the metabolic activity and cell membrane integrity (viability), this study demonstrated an impact of GP-concentration on these values. WST-1 confirmed a close relation between the increase of the GP-concentration and a significant decrease of the cell metabolic activity. However, cells seeded on top of non-cross-linked FAH also showed a reduction of these values as compared to 2D culture conditions. The quantification of the DNA released into the culture media, which it is considered a feasible method to determine irreversible cell-membrane damage due to exposure of cytotoxic agents [8, 23], suggest a concentration-dependent cytotoxicity of GP, especially when GP was used at 0.75%.

Overall *in vitro* biocompatibility characterization of our GP cross-linked FA-based hydrogels suggests a concentration-dependent cytotoxic effect of GP. In this context, the reduction of the viable cells density and metabolic activity and the increase of the DNA-released, especially when GP 0.75% was used, could be related to a concentration-dependent cytotoxicity of GP as previously suggested [19, 31, 32]; to a continuous release of active GP-molecules (which could interact with cell surface and cytoskeletal proteins) from the biomaterial [36], especially at higher concentration has occurred with GL [8]; or because GP-covalent molecular bonds could compromise the fibrin's motif related to the cell attachment. However, DNA quantitative analysis disclosed that the percentage of DNA released in FAH cross-linked with GP 0.75% was significantly lower (13.6%) than the negative control, where cells were exposed to an cytotoxic agent (100%), demonstrating a partial cytotoxic effect of GP at this higher concentration. If we compare the *in vitro* biocompatibility of FAH cross-linked with GP or GL, GP was considerably more biocompatible, even at higher concentrations. The best GL-cross-linked FA-based hydrogels resulted to be more cytotoxic than all concentrations of GP used in this study. Indeed, with the use of GL the

percentage of DNA released closely reach to the 80% [8]. Furthermore, this study was conducted with fibroblast obtained from primary cultures, and it is well-known that primary cultures are more sensible to toxic agents and changes on their microenvironment as compared to specific cell lines. Finally, the partial cytotoxic effect of GP should be considered within the structural and biomechanical properties of the scaffolds generated. However, degradation and *in vivo* studies are still needed in order to demonstrate the suitability of these novel cross-linked FAH and NFAH in tissue engineering.

In conclusion, this *ex vivo* study demonstrated that the generation of different scaffolds based on the use of FAH by using two bio-fabrication processes -GP cross-linking and nanostructuration- allowed us to generate versatile tissues-like scaffolds with customized structural properties (porosity and fiber density) and biomechanical properties. Furthermore, GP turned out to be an efficient cross-linking agent to significantly improve the stiffness, elasticity and viscosity of FAH and NFAH. In addition, our biocompatibility analyses confirmed a partial concentration-dependent cytotoxic of GP, especially at 0.75%, when the cell function and viability started to be compromised. Finally, based on our structural, rheological and biocompatibility characterization of GP cross-linked FA-based hydrogels, the use of GP concentrations between 0.1% to 0.5% demonstrated to be effective enough to improve the biomechanical properties and maintain an acceptable degree of *in vitro* biocompatibility, especially NFAH cross-inked with 0.5%. Finally, GP resulted to be an efficient alternative to the use of GL to generate mechanically stable and biocompatible FA-based hydrogels for different tissue engineering applications. However, further studies are still needed to elucidate the regenerative potential, biocompatibility and degradation-rate of these biomaterials *in vivo*.

Acknowledgments

This study was supported by the following research projects: Grant FIS PI14/1343 from the “Plan Nacional de Investigación Científica, Desarrollo e innovación Tecnológica (I+D+I) del Ministerio de Economía y Competitividad, España (Institutos de Salud Carlos III)”, co-financed by FEDER, European Union. Grant SAS PI-400-2016 from the “Fundación Progreso y Salud, Junta de Andalucía, España”. This work is part of the PhD thesis prepared by Gerson Vizcaino. The authors thank Dr. Ariane Ruyffelaert for the language assistance.

Competing interests

All authors declare there is not any financial or personal relationship with organizations that could potentially be perceived as influencing the described research.

References

[1] D. F. Williams. The biomaterials conundrum in tissue engineering. *Tissue Eng Part A*, 20(7-8):1129–31, 2014.

[2] G. Scionti, M. Moral, M. Toledano, R. Osorio, J. D. Duran, M. Alaminos, A. Campos, and M. T. Lopez-Lopez. Effect of the hydration on the biomechanical properties in a fibrin-agarose tissue-like model. *J Biomed Mater Res A*, 102(8):2573–82, 2014.

[3] C. Van Blitterswijk, P. Thomsen, A Lindahl, J. Hubbel, D. F. Williams, R Cancedda, J.D. De Bruijn, and J. Sohier. Natural polymers in tissue engineering aplications. *Tissue Eng*, pages 145–192, 2008.

[4] B. V. Slaughter, S. S. Khurshid, O. Z. Fisher, A. Khademhosseini, and N. A. Peppas. Hydrogels in regenerative medicine. *Adv Mater*, 21(32-33):3307–29, 2009.

[5] L. T. Vu, G. Jain, B. D. Veres, and P. Rajagopalan. Cell migration on planar and three-dimensional matrices: a hydrogel-based perspective. *Tissue Eng Part B Rev*, 21(1):67–74, 2015.

[6] R Brown, M Wiseman, CB Chuo, U Cheema, and S Nazhat. Ultra-rapid engineering of biomimetic tissues: a plastic compression fabrication process for nano-micro structures. *Adv. Funct. Mater.*, 15:1762–1770, 2005.

[7] N. Reddy, R. Reddy, and Q. Jiang. Crosslinking biopolymers for biomedical applications. *Trends Biotechnol*, 33(6):362–9, 2015.

[8] F. Campos, A. B. Bonhome-Espinosa, L. Garcia-Martinez, J. D. Duran, M. T. Lopez-Lopez, M. Alaminos, M. C. Sanchez-Quevedo, and V. Carriel. Ex vivo characterization of a novel tissue-like cross-linked fibrin-agarose hydrogel for tissue engineering applications. *Biomed Mater*, 11(5):055004, 2016.

[9] V. Carriel, G. Scionti, F. Campos, O. Roda, B. Castro, M. Cornelissen, I. Garzon, and M. Alaminos. In vitro characterization of a nanostructured fibrin agarose bio-artificial nerve substitute. *J Tissue Eng Regen Med*, 11(5):1412–1426, 2017.

[10] T. C. Gamboa-Martinez, V. Luque-Guillen, C. Gonzalez-Garcia, J. L. Gomez Ribelles, and G. Gallego-Ferrer. Crosslinked fibrin gels for tissue engineering: two approaches to improve their properties. *J Biomed Mater Res A*, 103(2):614–21, 2015.

[11] M. Alaminos, M. Del Carmen Sanchez-Quevedo, J. I. Munoz-Avila, D. Serrano, S. Medialdea, I. Carreras, and A. Campos. Construction of a complete rabbit cornea substitute using a fibrin-agarose scaffold. *Invest Ophthalmol Vis Sci*, 47(8):3311–7, 2006.

[12] M. C. Sanchez-Quevedo, M. Alaminos, L. M. Capitan, G. Moreu, I. Garzon, P. V. Crespo, and A. Campos. Histological and histochemical evaluation of human oral mucosa constructs developed by tissue engineering. *Histol Histopathol*, 22(6):631–40, 2007.

[13] V. Carriel, M. Alaminos, I. Garzon, A. Campos, and M. Cornelissen. Tissue engineering of the peripheral

nervous system. *Expert Rev Neurother*, 14(3):301–18, 2014.

[14] V. Carriel, J. Garrido-Gomez, P. Hernandez-Cortes, I. Garzon, S. Garcia-Garcia, J. A. Saez-Moreno, M. Del Carmen Sanchez-Quevedo, A. Campos, and M. Alaminos. Combination of fibrin-agarose hydrogels and adipose-derived mesenchymal stem cells for peripheral nerve regeneration. *J Neural Eng*, 10(2):026022, 2013.

[15] V. Carriel, I. Garzon, J. M. Jimenez, A. C. Oliveira, S. Arias-Santiago, A. Campos, M. C. Sanchez-Quevedo, and M. Alaminos. Epithelial and stromal developmental patterns in a novel substitute of the human skin generated with fibrin-agarose biomaterials. *Cells Tissues Organs*, 196(1):1–12, 2012.

[16] L. Garcia-Martinez, F. Campos, C. Godoy-Guzman, M. Del Carmen Sanchez-Quevedo, I. Garzon, M. Alaminos, A. Campos, and V. Carriel. Encapsulation of human elastic cartilage-derived chondrocytes in nanostructured fibrin-agarose hydrogels. *Histochem Cell Biol*, 147(1):83–95, 2017.

[17] R. Fernandez-Valades-Gamez, I. Garzon, E. Liceras-Liceras, A. Espana-Lopez, V. Carriel, M. A. Martin-Piedra, M. A. Munoz-Miguelsanz, M. C. Sanchez-Quevedo, M. Alaminos, and R. Fernandez-Valades. Usefulness of a bioengineered oral mucosa model for preventing palate bone alterations in rabbits with a mucoperiostial defect. *Biomed Mater*, 11(1):015015, 2016.

[18] A. Bigi, G. Cojazzi, S. Panzavolta, K. Rubini, and N. Roveri. Mechanical and thermal properties of gelatin films at different degrees of glutaraldehyde crosslinking. *Biomaterials*, 22(8):763–8, 2001.

[19] E. V. Dare, M. Griffith, P. Poitras, J. A. Kaupp, S. D. Waldman, D. J. Carlsson, G. Dervin, C. Mayoux, and M. T. Hincke. Genipin cross-linked fibrin hydrogels for in vitro human articular cartilage tissue-engineered regeneration. *Cells Tissues Organs*, 190(6):313–25, 2009.

[20] M. E. McGann, C. M. Bonitsky, M. L. Jackson, T. C. Ovaert, S. B. Trippel, and D. R. Wagner. Genipin crosslinking of cartilage enhances resistance to biochemical degradation and mechanical wear. *J Orthop Res*, 33(11):1571–9, 2015.

[21] V. Carriel, I. Garzon, A. Campos, M. Cornelissen, and M. Alaminos. Differential expression of gap-43 and neurofilament during peripheral nerve regeneration through bio-artificial conduits. *J Tissue Eng Regen Med*, 11(2):553–563, 2017.

[22] A. B. Bonhome-Espinosa, F. Campos, I. A. Rodriguez, V. Carriel, J. A. Marins, A. Zubarev, J. D. Duran, and M. T. Lopez-Lopez. Effect of particle concentration on the microstructural and macromechanical properties of biocompatible magnetic hydrogels. *Soft Matter*, 2017.

[23] L. Rodriguez-Arco, I. A. Rodriguez, V. Carriel, A. B. Bonhome-Espinosa, F. Campos, P. Kuzhir, J. D. Duran, and M. T. Lopez-Lopez. Biocompatible magnetic core-shell nanocomposites for engineered magnetic tissues. *Nanoscale*, 8(15):8138–50, 2016.

[24] Chi Ninh, Aimon Iftikhar, Madeline Cramer, and Christopher J Bettinger. Diffusion–reaction models of genipin incorporation into fibrin networks. *Journal of Materials Chemistry B*, 3(22):4607–4615, 2015.

[25] Ramavatar Meena, Kamalesh Prasad, and AK Siddhanta. Preparation of genipin-fixed agarose hydrogel. *Journal of applied polymer science*, 104(1):290–296, 2007.

[26] U. Cheema, T. Alekseeva, E. A. Abou-Neel, and R. A. Brown. Switching off angiogenic signalling: creating channelled constructs for adequate oxygen delivery in tissue engineered constructs. *Eur Cell Mater*, 20:274–80; discussion 280–1, 2010.

[27] M. Geerligs, C. Oomens, P. Ackermans, F. Baaijens, and G. Peters. Linear shear response of the upper skin layers. *Biorheology*, 48(3-4):229–45, 2011.

[28] L. M. Delgado, Y. Bayon, A. Pandit, and D. I. Zeugolis. To cross-link or not to cross-link? cross-linking associated foreign body response of collagen-based devices. *Tissue Eng Part B Rev*, 21(3):298–313, 2015.

[29] M. Stolz, R. Raiteri, A. U. Daniels, M. R. VanLandingham, W. Baschong, and U. Aebi. Dynamic elastic modulus of porcine articular cartilage determined at two different levels of tissue organization by indentation-type atomic force microscopy. *Biophys J*, 86(5):3269–83, 2004.

[30] C. Meyer, L. Stenberg, F. Gonzalez-Perez, S. Wrobel, G. Ronchi, E. Udina, S. Suganuma, S. Geuna, X. Navarro, L. B. Dahlin, C. Grothe, and K. Haastert-Talini. Chitosan-film enhanced chitosan nerve guides for long-distance regeneration of peripheral nerves. *Biomaterials*, 76:33–51, 2016.

[31] F. Mwale, M. Iordanova, C. N. Demers, T. Steffen, P. Roughley, and J. Antoniou. Biological evaluation of chitosan salts cross-linked to genipin as a cell scaffold for disk tissue engineering. *Tissue Eng*, 11(1-2):130–40, 2005.

[32] G. Fessel, J. Cadby, S. Wunderli, R. van Weeren, and J. G. Snedeker. Dose- and time-dependent effects of genipin crosslinking on cell viability and tissue mechanics - toward clinical application for tendon repair. *Acta Biomater*, 10(5):1897–906, 2014.

[33] R. J. Errington, K. Puustjarvi, I. R. White, S. Roberts, and J. P. Urban. Characterisation of cytoplasm-filled processes in cells of the intervertebral disc. *J Anat*, 192 (Pt 3):369–78, 1998.

[34] H. G. Sundararaghavan, G. A. Monteiro, N. A. Lapin, Y. J. Chabal, J. R. Miksan, and D. I. Shreiber. Genipin-induced changes in collagen gels: correlation of mechan-

ical properties to fluorescence. *J Biomed Mater Res A*, 87(2):308–20, 2008.

[35] R. M. Schek, A. J. Michalek, and J. C. Iatridis. Genipin-crosslinked fibrin hydrogels as a potential adhesive to augment intervertebral disc annulus repair. *Eur Cell Mater*, 21:373–83, 2011.

[36] C. Wang, T. T. Lau, W. L. Loh, K. Su, and D. A. Wang. Cytocompatibility study of a natural biomaterial crosslinker–genipin with therapeutic model cells. *J Biomed Mater Res B Appl Biomater*, 97(1):58–65, 2011.